

Supporting Information

Visible-light Photocatalytic Hydrogen Production in A Narrow-bandgap Semiconducting La/Ni-modified KNbO₃ Ferroelectric and Further Enhancement via High-field Poling

Wenbin Tang¹, Xiaogang Xue¹, Changlai Yuan^{†, 1, 2}, Jun Chen^{†, 2}, Lei Miao^{1, 3}, Qin Feng⁴, Jiwen Xu¹, Guanghui Rao^{†, 1}, Jiang Wang¹, Changrong Zhou¹, Yiping Guo[†]

5

¹ Guangxi Key Laboratory of Information Materials, School of Material Science and Engineering, Guilin University of Electronic Technology, Guilin 541004, China

² School of Mathematics and Physics, University of Science and Technology Beijing, Beijing 100083, China

³ Department of Materials Science and Engineering, SIT Research Laboratories, Innovative Global Program, Faculty of Engineering, Shibaura Institute of Technology, Tokyo 1358548, Japan

⁴ School of Resources, Environment and Materials, Guangxi University, Nanning 530004, China

⁵ State Key Laboratory of Metal Matrix Composites, School of Materials Science and Engineering, Shanghai Jiao Tong University, Shanghai 200240, China

†Corresponding authors. Changlai Yuan, Email: yuanchanglai@guet.edu.cn

Jun Chen, Email: junchen@ustb.edu.cn

Guanghui Rao, Email: rgh@guet.edu.cn

Yiping Guo, Email: ypguo@sjtu.edu.cn

Table S1. Unit cell parameters of (1-x) KN-xLN ceramics (x = 0.00–0.04) via refinement analysis

Parameters	x = 0.00	x = 0.01	x = 0.02		x = 0.03		x = 0.04		
Sig	1.01	1.21	1.38		1.86		1.54		
R _{wp} (%)	7.6	7.9	8.4		9.2		8.6		
R _b (%)	10.5	11.4	11.8		12.3		11.9		
Space group	Amm2	Amm2	P4mm	Amm2	P4mm	Amm2	P4mm	Amm2	P4mm
Symmetry	O phase	O phase	T phase	O phase	T phase	O phase	T phase	O phase	T phase
Phase fraction (%)	100	95.61	4.39	93.81	6.19	91.49	8.51	89.92	10.18
a (Å)	4.0040(0)	3.9902(5)	4.0584(8)	4.0012(1)	4.0398(1)	4.0005(5)	4.0444(5)	4.0078(8)	3.9549(8)
b (Å)	5.6817(0)	5.6791(6)	4.0584(8)	5.6763(0)	4.0398(1)	5.6930(2)	4.0444(5)	5.6717(7)	3.9549(9)
c (Å)	5.7040(0)	5.6935(6)	4.0704(1)	5.6870(3)	4.0616(0)	5.6749(1)	4.0605(9)	5.6680(0)	4.0520(5)
c/a	1.4246	1.4268	1.0029	1.4213	1.0053	1.4185	1.0039	1.4142	1.0245
c/b	1.0039	1.0025	1.0029	1.0018	1.0053	0.9968	1.0039	0.9993	1.0245
α=β=γ (°)	90	90	90	90	90	90	90	90	90
Z	2	2	1	2	1	2	1	2	1
V (Å ³)	129.7633	129.0234	67.0449	129.1645	66.2858	129.2476	66.4217	128.8441	63.3822
δ	0.0039	0.0025	0.0029	0.0018	0.0053	0.0032	0.0039	0.0007	0.0245
Atomic positions									
A atomic (x, y, z)	(0, 0, 0.01380)	(0, 0, 0.04216)	(0, 0, 2.18600)	(0, 0, 0.00699)	(0, 0, 0.95489)	(0, 0, 0.04766)	(0, 0, 2.31954)	(0, 0, -0.08279)	(0, 0, 2.21600)
B atomic (x, y, z)	(0.5, 0, 0.5)	(0.5, 0.56051)	(0.5, 1.66769)	(0.5, 0.52984)	(0.5, 0.65545)	(0.5, 0.56546)	(0.5, 1.69745)	(0.5, 0.43691)	(0.5, 1.70769)
O ₁ (x, y, z)	(0, 0, 0.53640)	(0, 0, 0.60503)	(0.5, 0.5, 3.06799)	(0, 0, 0.58847)	(0.5, 0.5, 0.99635)	(0, 0, 0.59546)	(0.5, 0.5, 3.06682)	(0, 0, 0.49480)	(0.5, 0.5, 3.06690)
O ₂ (x, y, z)	(0.5, 0.24760, 0.28420)	(0.5, 0.22269, 0.28051)	(0.5, 0.20965, 3.93449)	(0.5, 0.20965, 0.25060)	(0.5, 0.82920, 0.27815)	(0.5, 0.21529, 0.27815)	(0.5, 0.21529, 3.90580)	(0.5, 0.21211, 0.16024)	(0.5, 0, 3.91112)

First principles calculation

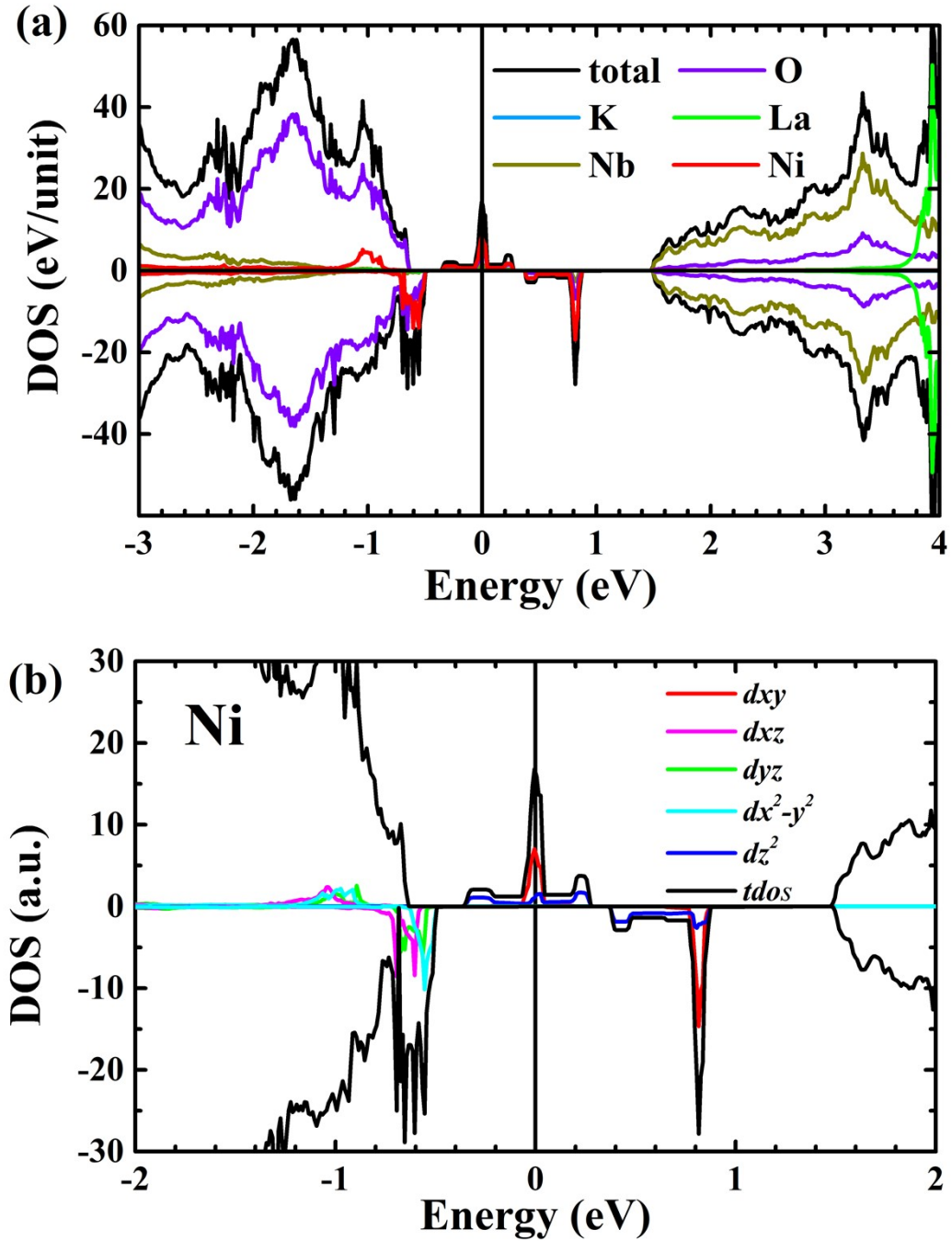


Figure S1 (a) Density of states of 0.96KN-0.04LN unit cell, where Ni 3d functions as the midgap state between valence band maximum and conduction band minimum; (b) partial density of states of Ni 3d. In Figure S1a, an apparent midgap state of Ni 3d between VBM and CBM is observed in spin-down channels. The formation of NiO₅ complex induces additional splitting between d_{z^2} and $d_{x^2-y^2}$ orbitals of double-degenerate states e_g as well as d_{xy} and $d_{xz/yz}$ orbitals of threefold-degenerate states t_{2g} [1].

A partial DOS calculation of spin-down Ni 3d state (Figure S1b) shows that the e_g state splits into half-filled d_z^2 and $d_{x^2-y^2}$, and t_{2g} splits into filled states of d_{xy} and $d_{xz/yz}$. The calculation simultaneously demonstrates that interband transitions of three absorption peaks are derived from Ni $3d_{x^2-y^2} \rightarrow Ni\ 3d_z^2 \rightarrow Ni\ 3d_{xy}$ transitions. When the photon energy reaches ~ 1.4 eV, the electrons can be excited from VBM to Ni $3d_z^2$. Lower at ~ 0.6 eV, the electrons in Ni $3d_z^2$ orbital can have a transition to CBM. If photon energy of ~ 2.0 eV in light irradiation is sufficiently absorbed, electrons of materials can be directly excited from VBM to CBM.

XPS analysis and specific surface area

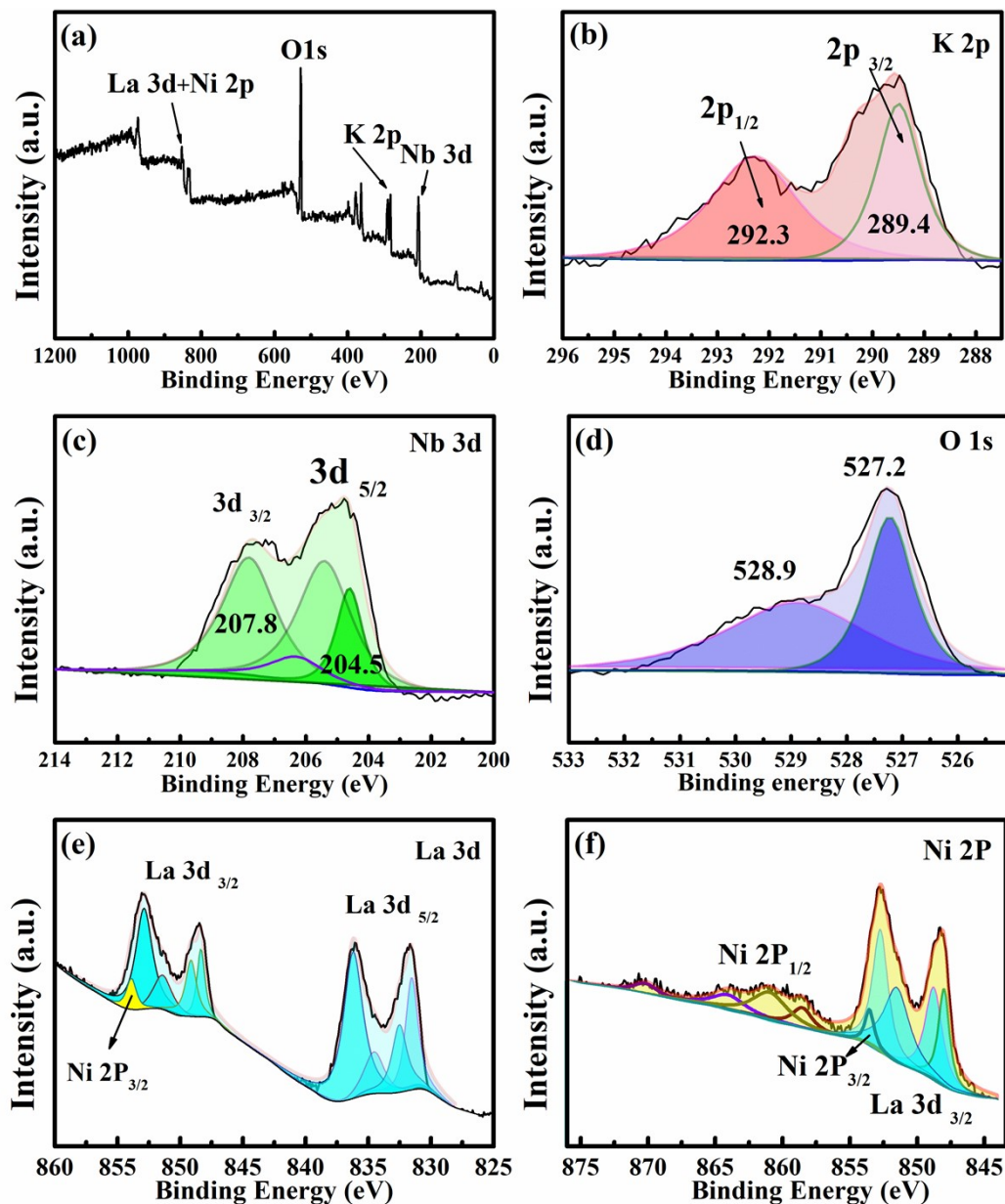


Figure S2 XPS spectra for (a) survey spectrum, (b) K 2P, (c) Nb 3d, (d) O 1s, (e) La 3d, and (f) Ni 2p of the 0.96KN-0.04LN ceramic. XPS spectra of the semiconducting 0.96KN-0.04LN sample are shown in Figure. S2a-f. As shown in Figure S2a, survey spectra confirm that K, Nb, O, La, and Ni elements exist in the sample. As shown in Figure S2b, two characteristic K2p_{3/2} and 2p_{1/2} peaks at 292.3 and 289.4 eV prove that K is in the +1 valence state. As shown in Figure S2c, two characteristic Nb 3d peaks located at 204.5 and 207.8 eV can be ascribed to Nb⁵⁺ corresponding to the reported values in KNbO₃ [2]. O 1s spectra (Figure S2d) can be

divided into the following: (1) the peak at 527.2 eV is associated with the lattice oxygen at and (2) the peak at 528.9 eV is associated with oxygen vacancies at around [3, 4]. As shown in Figure S2e, two pairs of peaks located at 831.6 (836.0 eV) and 848.5.8 (852.9 eV) eV are individually determined as $\text{La}^{3+} 3d_{5/2}$ and $\text{La}^{3+} 3d_{3/2}$, respectively. The Ni $2p_{3/2}$ peak, which overlaps with the La $3d_{3/2}$ peak (Figure. S2e and S2f), can be deconvoluted to the center at 853.9 eV, thereby indicating that the chemical state of Ni is +2. Three peaks located at 858.5, 861.0, and 864.0 eV can be assigned to Ni $2p_{1/2}$, thereby suggesting the +3 valance state of Ni. These findings are consistent with the results in the literature [4-6]. **When Nb^{5+} ions are replaced by Ni^{2+} ions, oxygen vacancy defects are formed in the 0.96KN–0.04LN lattice to maintain electric neutrality.** This result also revealed that the 0.96KN–0.04LN is defect-induced narrow-bandgap ferroelectric semiconductors. This result is similar to the findings in the literature [7, 8]. The ratio of Ni^{2+} and Ni^{3+} is estimated at 1:5.4 according to the ratio of peak area obtained from the fitting results. Therefore, the theoretical value of oxygen deficiency (δ) of the doping composition $\text{LaNiO}_{3-\delta}$ is 0.08 and the specific formula of the 0.96KN–0.04LN sample is expressed as $(\text{K}_{0.96}\text{La}_{0.04})(\text{Nb}_{0.96}, \text{Ni}_{0.04})\text{O}_{2.92}$.

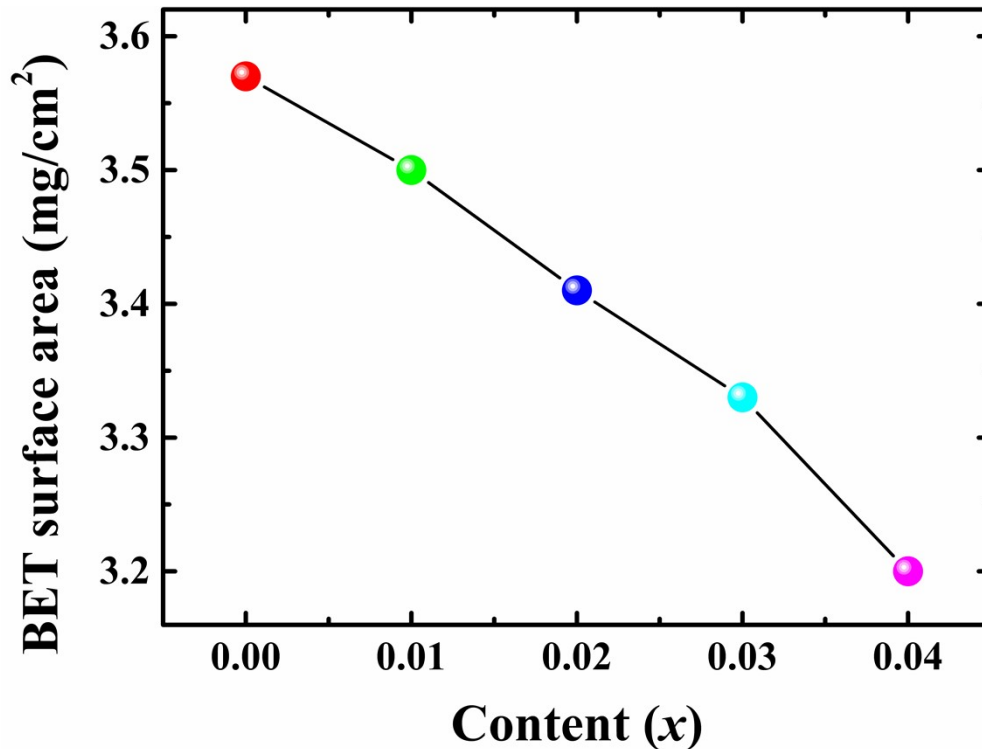


Figure S3 Specific surface area of $(1-x)\text{KN}-x\text{LN}$ ($x = 0.00-0.04$) ceramics

References

- [1] C.Q. Li, F. Wang, Y.Y. Sun, K. Jiang, S.J. Gong, Z.G. Hu, Z.Y. Zhou, X.L. Dong and J.H. Chu, *Phys. Rev. B*, 2018, **97**, 094109.
- [2] S. Si, H. Deng, W. Zhou, T. Wang, P. Yang and J. Chu, *Ceram. Int.*, 2018, **44**, 14638-14644.
- [3] Z. Chen, C. Yuan, X. Liu, L. Meng, S. Cheng, J. Xu, C. Zhou, J. Wang and G. Rao, *Mater. Sci. Semicond. Process*, 2020, **115**, 105089.
- [4] J. L. Lin, Z.J. Wang, X. Zhao and Z.D. Zhang, *Scr. Mater.*, 2020, **179**, 102-106.
- [5] X. Zhou, Y. Chen, C. Li, L. Zhang, X. Zhang, X. Ning, L. Zhan and J. Luo, *Sep. Purif. Technol.*, 2019, **211**, 179-188.
- [6] S. Yao, R. Zheng, R. Li, Y. Chen, X. Zhou and J. Luo, *J. Taiwan Inst. Chem. E*, 2019, **100**, 186-193.
- [7] I. Grinberg, D.V. West, M. Torres, G. Gou, D.M. Stein, L. Wu, G. Chen, E.M.

Gallo, A.R. Akbashev, P.K. Davies, J.E. Spanier and A.M. Rappe, Perovskite oxides for visible-light-absorbing ferroelectric and photovoltaic materials, *Nature*, 2013, **503**, 509-512.

[8] S. Chakraborty, and S. Mukherjee, *J. Aust. Ceram. Soc.*, 2017, **53**, 701-711.